Open access • Journal Article • DOI:10.1143/JJAP.45.6071

Grating Couplers for Coupling between Optical Fibers and Nanophotonic Waveguides — Source link

Dirk Taillaert, Frederik Van Laere, M. Ayre, Wim Bogaerts ...+3 more authors

Institutions: Ghent University, University of St Andrews

Published on: 04 Aug 2006 - Japanese Journal of Applied Physics (IOP Publishing)

Topics: Grating, Optical fiber, Photonics and Nanophotonics

Japanese Journal of Applied Physics
Vol. 45, No. 8A, 2006, pp. 6071–6077

Invited Paper

Grating Couplers for Coupling between Optical Fibers and Nanophotonic Waveguides

Dirk TAILLAERT*, Frederik VAN LAERE, Melanie AYRE[1], Wim BOGAERTS, Dries VAN THOURHOUT, Peter BIENSTMAN and Roel BAETS

Photonics Research Group, Department of Information Technology, Ghent University, Sint-Pietersnieuwstraat 41, 9000 Gent, Belgium
[1]*School of Physics and Astronomy, University of St. Andrews, St. Andrews, Fife, KY16 9SS, U.K.*

(Received February 15, 2006; accepted April 17, 2006; published online August 4, 2006)

Nanophotonic waveguides and components are promising for use in the large-scale integration of photonic circuits. Coupling light between nanophotonic waveguides and a single-mode fiber is an important problem and many different solutions have been proposed and demonstrated in recent years. In this paper, we discuss a grating coupler approach. Grating couplers can be placed anywhere on a circuit and can easily be integrated. We have experimentally demonstrated >30% coupling efficiency with a 1 dB bandwidth of 40 nm on standard wafers. Theoretically, the coupling efficiency can be improved to >90% using an optimized grating design and layer stack. The fabrication of the couplers in silicon-on-insulator and in indium phosphide membranes is also discussed. [DOI: 10.1143/JJAP.45.6071]

KEYWORDS: grating coupler, silicon-on-insulator, integrated optics, nanophotonics, indium phosphide

1. Introduction

Materials with a high refractive index contrast are useful for high-density photonic integrated circuits. The basic building blocks of those circuits are nanophotonic waveguides such as photonic-crystal or photonic-wire waveguides. Examples of materials with a high refractive index contrast are silicon-on-insulator (SOI) or indium phosphide (InP) membranes with an air cladding. However, a difficulty is coupling light between optical fibers and integrated waveguides. Because the waveguide core layer is only 100–300 nm thick and the guided mode is strongly confined in that core, there is a large mismatch between the waveguide mode and a single-mode fiber mode. This coupling problem is important and several groups have recently demonstrated[1,2] coupling losses below 1 dB using an inverted lateral taper with a polymer overlay. Although this is a very elegant solution to the coupling problem, it may be beneficial to have a surface coupler that can be placed anywhere on a chip, not only at the edges. Such a coupler does not require polishing of facets and allows wafer-scale testing of photonic integrated circuits because light can be coupled in and out of the surface of the chip. Waveguide grating couplers are suitable for this task.

The use of grating couplers to couple light into thin-film waveguides is well known.[3–5] However, when conventional gratings with a small coupling strength are used, long gratings are needed, and the outcoupled beam is much larger than the fiber mode. As a result, an additional lens is needed to couple to a fiber[4] or, alternatively, a curved grating can be used[6] that focuses the light into a fiber. We use a very short grating with a large coupling strength, and the fiber is butt-coupled to this grating.[7] This is schematically shown in Fig. 1. This approach results in a relatively large bandwidth. Also, the fabrication and packaging are straightforward because no lenses are needed. The grating coupler can be fabricated using one additional lithography and etching step. Standard single-mode fibers and fiber arrays can be used for the packaging. The grating, which couples light from an out-of-plane fiber into a planar waveguide, is followed by an in-plane taper to couple to a single-mode photonic wire waveguide (Fig. 1).

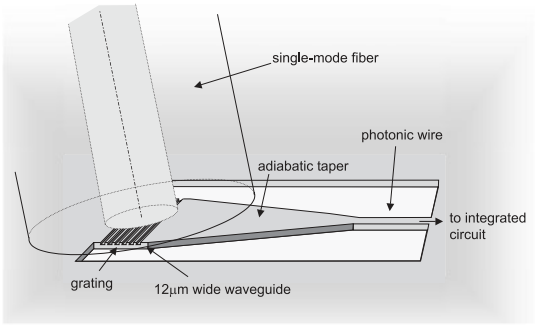

Fig. 1. Principle of grating coupler for coupling between photonic wire waveguide and fiber.

In §2, we will discuss the design of the coupler. In §3 and §4, the experimental results of SOI and InP-membrane waveguides are presented. All the results given in this paper are for TE polarization (transverse electric field, E-field parallel to the grating grooves). Because the grating couplers are polarization sensitive, the structures in this paper are only appropriate for polarization-controlled applications such as interconnects and sensors. For use in optical communications, a polarization diversity configuration is needed. In this configuration, a two-dimensional or crossed grating may be used as a polarization splitter.[8]

2. Design of Grating Coupler

2.1 Introduction

The basic grating structure is a periodic structure with a finite number of rectangular grating teeth. The grating period for vertical out-of-plane coupling is $\Lambda = \lambda/n_{\mathrm{eff}}$. Only in the case of a weak perturbation grating is n_{eff} the effective index of the unperturbed waveguide mode, otherwise this index must be calculated. Unfortunately, when light from a grating coupler leaves a waveguide at 90° there is also a second-

*E-mail address: dirk.taillaert@intec.ugent.be

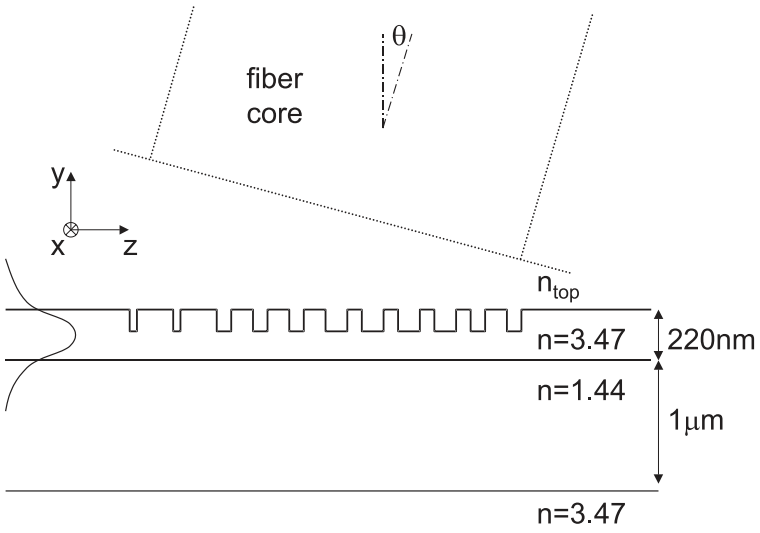

Fig. 2. Simulation model used for calculation of coupling efficiency.

order diffraction which reflects light back into the waveguide. To avoid this unwanted second order reflection, the grating is typically detuned and the light is coupled out at a small angle with respect to the surface normal direction. In this paper, we call this angle θ. Although several numerical methods[9] and approximate expressions[10] exist to calculate the efficiency of grating couplers, we have used a more general numerical method, the eigenmode expansion method, because it can also be applied to nonperiodic structures. We calculate the coupling efficiency from the waveguide to the fiber. The coupling efficiency from the fiber to the waveguide is the same because the coupling between the two modes (single-mode fiber and waveguide) is considered.

The simulation model we have used is shown in Fig. 2. We modelled[7] the waveguide grating coupler using the eigenmode expansion method with perfectly matched layers (PML) boundary conditions.[11] This method yields the electromagnetic fields when the waveguide mode is incident on the grating. The coupling efficiency to the fiber is then calculated using an overlap integral with a Gaussian profile with a beam diameter of 10.4 μm. These calculations are two-dimensional (2-D) and for TE polarization. To obtain a three-dimensional (3-D) approximation, we take the finite waveguide width into account by multiplying the 2-D results with an overlap integral between the waveguide and the fiber in the x-direction. This method is described in detail in ref. 12 and is similar to the well-known effective index method. This approximation is valid because the waveguide width (typically 12 μm) is much larger than the wavelength used. We use a 220 nm thick silicon core and 1 μm oxide cladding as shown in Fig. 2. In the case of standard SOI, the top cladding layer is air ($n_{top} = 1$). In the high-refractive-index-contrast waveguide, there is a large difference between the effective index of the fundamental TE mode (2.83) and the fundamental TM mode (1.89). As a result, the grating coupler is strongly polarization selective. We have only considered the TE case in this paper.

2.2 *Basic grating*

To avoid second-order reflection at the waveguide-grating interface, the grating is detuned and light is coupled out at a small angle with respect to the vertical direction. An angle θ of 10° is chosen because it is sufficient to avoid reflection. After optimizing the grating period, filling factor and etch depth, the calculated coupling efficiency to the fiber is approximately 37% for an etch depth of 70 nm and a filling factor of 0.5. The grating period is $\Lambda = 630$ nm, which gives a central wavelength around $\lambda = 1550$ nm. Coupling efficiency as a function of wavelength is shown in Fig. 3. The 1 dB bandwidth of the coupler is approximately 40 nm. The unwanted reflection at the waveguide grating interface is less than −20 dB in this wavelength range. The calculated coupling length L_c of the grating is approximately 3.8 μm, which corresponds to the theoretical optimal coupling length calculated with the formula $w_0 = 1.37 L_c \cos(\theta)$ given in ref. 5. In Fig. 3, the total upwards coupled power is also shown. The coupling efficiency to fiber is lower than the upwards radiated power, because there is a mismatch between the fiber mode (Gaussian) and the outcoupled field, which approximately exponentially decays in the z-direction.

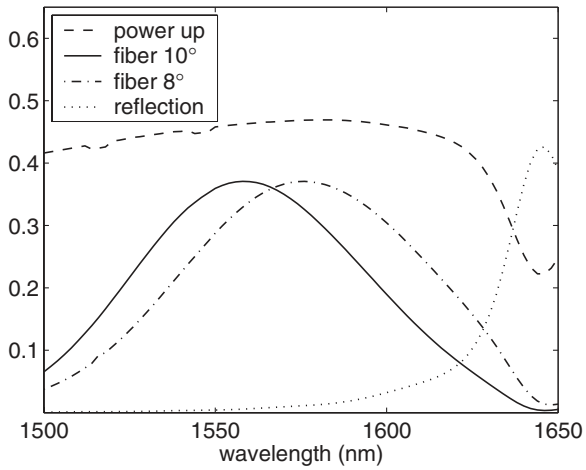

Fig. 3. Simulation result of uniform SOI grating. ($\Lambda = 630$ nm, etch depth = 70 nm, filling factor = 0.5.) The upwards radiated power, coupling efficiency to the fiber and reflection at the waveguide grating interface are plotted.

The coupling efficiency of this basic grating coupler is limited by two factors. First, the light coming from the waveguide is not only coupled upwards towards the fiber, but also downwards towards the substrate. Second, there is a mismatch between the field from a uniform grating and the fiber mode. These two problems and solutions are discussed in the next paragraphs.

2.3 Other layer stack

The easiest way to increase the coupling efficiency is to put a top cladding layer onto the silicon. This layer increases the up/down ratio of the outcoupled power. Also, if the refractive index of this top layer is equal to the effective index of the fiber, reflections at the fiber facet are avoided. With an index-matching layer ($n_{top} = 1.46$), the efficiency is increased to 44%. It should be noted that the coupling angle is also different from the case with an air top cladding. An angle of $\theta = 8^\circ$ is used to maintain the central wavelength at around 1550 nm.

Also, the thickness of the buried oxide layer is an important determinant of the coupling efficiency. A change in buried oxide thickness also changes the up/down ratio and the coupling strength of the grating.[3] For our grating parameters, the optimal thickness is 900 nm or 1.45 μm, resulting in an efficiency of 53%.

Even with the optimal buried oxide thickness, there is still some power coupled towards the substrate and lost. This can be avoided by adding a bottom reflector to the layer structure. The bottom reflector may be a multilayer dielectric reflector[13] or a gold mirror. A simulation with a two-pair Si/SiO_2 mirror results in a 79% coupling efficiency to the fiber. With the bottom reflector, no light is lost to the substrate, but the coupling efficiency is still limited. To increase this further, an optimized nonuniform grating has to be used. This is discussed in the next paragraph. The results presented in this paragraph are summarized in Table I and Fig. 4.

2.4 Nonuniform grating

A grating coupler with a uniform grating can have a maximum theoretical[5] coupling efficiency of approximately 80%, because the output beam has an exponentially decaying power $P = P_0 \exp(-2\alpha z)$ along the propagation direction. α is called the leakage factor or coupling strength of the grating. For a nonuniform grating, α becomes a function of z and the output beam can be shaped differently. To achieve a Gaussian output beam, $\alpha(z)$ is given[14,15] by

Table I. Calculated coupling efficiencies for uniform SOI grating couplers on different layer structures. The refractive index of the top cladding layer is n_{top}. The thickness of the buried oxide layer is th_{buffer}. The grating parameters used are $\Lambda = 630$ nm, the etch depth is 70 nm, and the filling factor 0.5.

Layer stack	th_{buffer} (μm)	n_{top}	Efficiency (%)
SOI	1	1	37
SOI with top cladding	1	1.46	44
SOI with optimal th_{buffer}	1.45	1.46	53
SOI with bottom mirror	1.47	1.46	79

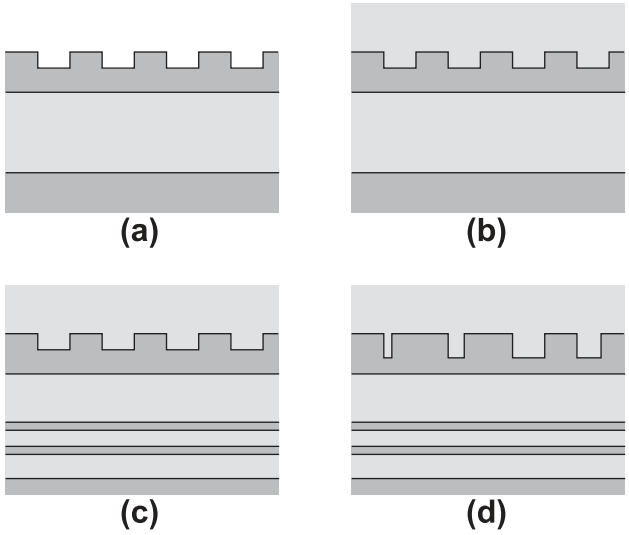

Fig. 4. Schematic drawing of different types of couplers: Uniform grating in (a) SOI with air top cladding, (b) SOI with oxide top cladding, (c) SOI with bottom Si/SiO_2 mirror. In (d), a grating coupler with varying groove widths is shown. Dark gray represents Si and light gray SiO_2.

$$2\alpha(z) = \frac{G^2(z)}{1 - \int_0^z G^2(t)\,dt} \tag{2.1}$$

where $G(z)$ is a normalized Gaussian profile with a beam diameter of 10.4 μm for coupling to the fiber. To achieve this z-dependence of α, either the etch depth[14] or the filling factor[15] of the grating can be varied. It should be noted that eq. (2.1) is only exact for a long grating with small α, which is not the case for our structure. Therefore, we use the results of eq. (2.1) as a starting point and perform a further numerical optimization for the grating structure. Details on the optimization can be found in ref. 12. It is found that for SOI with an optimized oxide buffer thickness (925 nm) the maximum coupling efficiency to the fiber is 61%. The relationship between efficiency and wavelength is shown in Fig. 5. The efficiency is limited because approximately 35% of light is lost to the substrate. The efficiency can be further

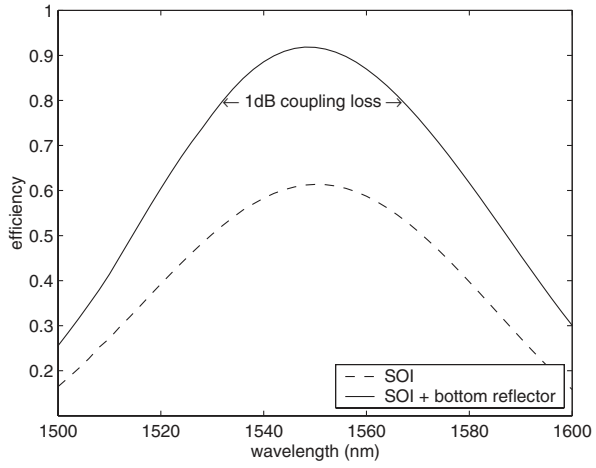

Fig. 5. Calculated coupling efficiency as function of wavelength for optimized grating coupler designs. For regular SOI, the maximum efficiency is 61%; for SOI with an additional bottom reflector, the maximum efficiency is 92%.

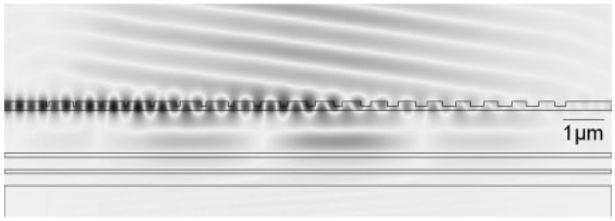

Fig. 6. Field plot of optimized structure with Si/SiO_2 bottom reflector. The E_x field is drawn.

improved using SOI with a bottom reflector. For SOI with a 2-pair Si/SiO_2 reflector under the waveguide, the maximum coupling efficiency after optimization is 92%. In this structure, only 2% is lost to the substrate. The other 98% is coupled upwards, but there is still a small mismatch with the fiber mode, which results in a maximum coupling efficiency of 92% to the fiber. The optimal grating parameters are also different for SOI and SOI with a bottom reflector, because the reflector influences not only the up/down ratio, but also the coupling strength of the grating. The optimal structure is shown in Fig. 6 together with a field plot. The depth of the grooves is 100 nm, the width of the smallest groove is only 30 nm and an index-matching layer is used as top cladding. The coupling loss to fiber for this structure is less than 1 dB in the wavelength range 1532–1567 nm (see Fig. 5). In this wavelength range the unwanted reflection at the waveguide grating interface is less than −24 dB.

2.5 *Alignment tolerances*

We will discuss the sensitivity to alignment errors in this paragraph. The tolerances for both angular (tilt) and positional alignment errors have been calculated. In these calculations, the fiber mode is approximated by a Gaussian beam with beam diameter of 10.4 μm.

Two different angles are considered. θ is the angle between the fiber and the vertical direction, projected on the yz-plane (Fig. 2). As discussed before, $\theta \neq 0^\circ$ to avoid reflection at the grating. When θ changes slightly, the central wavelength of the coupler spectrum changes. This wavelength shift is approximately 9 nm per degree. In Fig. 3, the coupling curves for an angle θ of 8 and 10° are shown. The second angle considered is ϕ as defined in the inset of Fig. 7. ϕ is the angle between the fiber and the vertical direction, projected on the xy-plane. In the case of optimal fiber alignment, $\phi = 0^\circ$. An error on ϕ reduces the coupling efficiency, as shown on Fig. 7. An error of 2° results in 0.5 dB additional coupling loss, but for larger angles, the coupling loss increases rapidly.

The effect of the distance between the fiber facet and the grating is determined by the diffraction of the Gaussian beam. A calculation result is shown in Fig. 8. In this calculation, an index-matching layer ($n = 1.46$) is used between the grating and the fiber. For a distance below 15 μm, the additional coupling loss is negligible. The additional loss is 0.5 dB for a distance of 55 μm. Finally, we consider the tolerances to lateral alignment errors. The fiber position is changed in the xz-plane and the distance between the fiber and the grating is 10 μm. In Fig. 9, the contour plot shows the additional coupling loss caused by lateral alignment

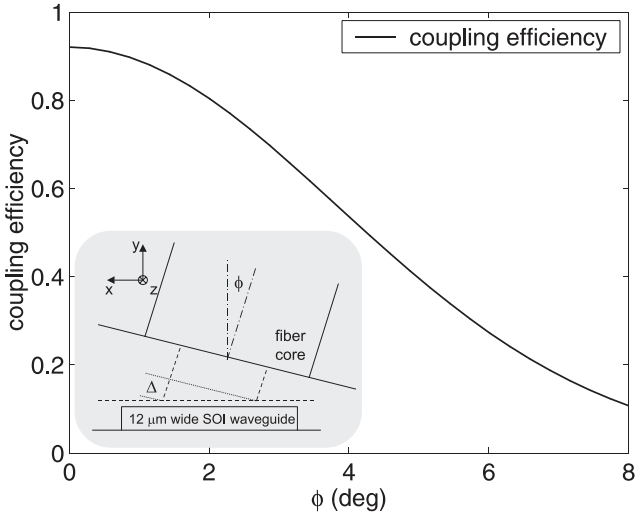

Fig. 7. Angular alignment tolerances. The coupling efficiency is shown for the coupler of Fig. 6 as a function of the angle ϕ. ϕ is the angle between the fiber and surface normal, projected on the xy-plane.

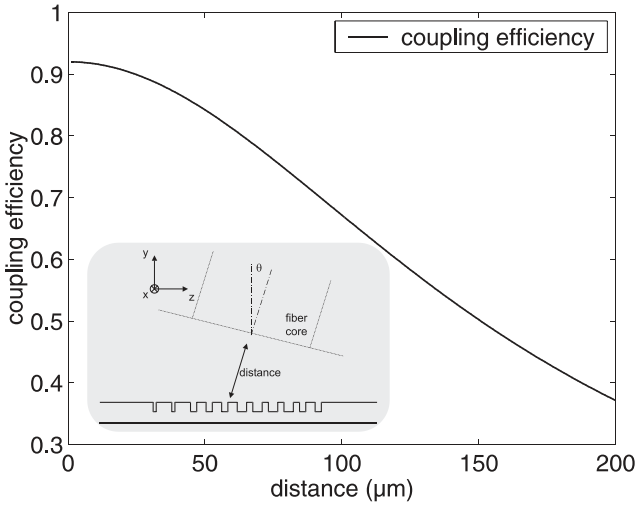

Fig. 8. Calculated coupling efficiency for the coupler of Fig. 6 as a function of the distance between fiber and grating.

errors. The simulation results are the smooth curves in the figure. An alignment error of 1 μm in any direction results in less than 0.5 dB additional coupling loss.

2.6 *Refractive index contrast*

The compact couplers we have described, only work well in a waveguide with a high refractive index contrast between the waveguide core and the cladding. In the case of SOI material, this index contrast is approximately 3.5 : 1.5. Because of the high vertical index contrast, the mode is well confined in the waveguide core and a high coupling strength can be achieved using a rather shallow grating (e.g., the coupling length $L_c = 3.8$ μm in the example given in §2.2 was achieved using a 70 nm deep grating). Also the high contrast results in a high reflectivity of the Si/SiO_2 interfaces. This high reflectivity allows an increase in directionality (up/down ratio) and thus also increases the efficiency of the grating coupler when the layer thickness is optimized.

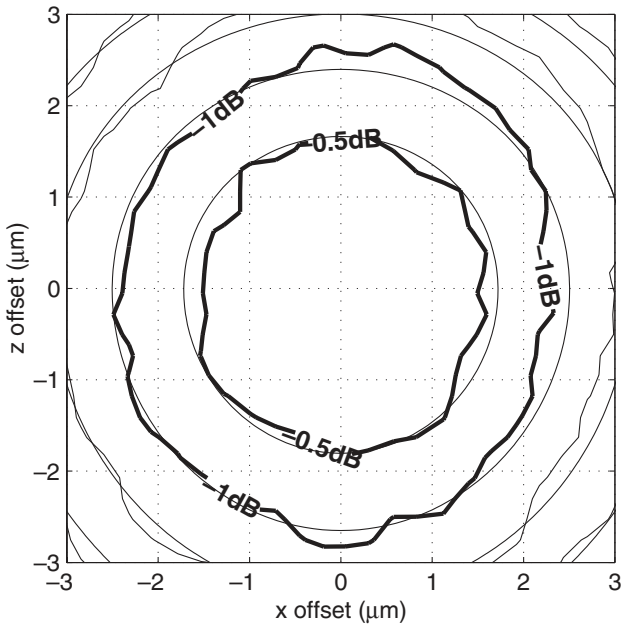

Fig. 9. Comparison of simulation and measurement results of the lateral alignment tolerances. The smooth curves are simulation results. The normalized coupling efficiency is shown as function of the lateral position of the fiber. The distance between fiber and grating is approximately 10 μm. The −0.5 and −1 dB contour are indicated on the figure.

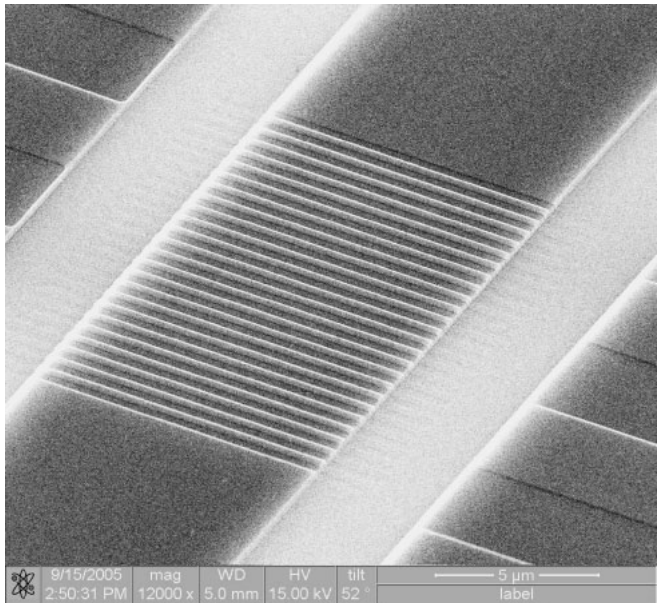

Fig. 10. SEM view of couplers fabricated using deep UV lithography. The depth of the grating grooves is 70 nm, the depth of the waveguide trenches is 220 nm.

Waveguides made in conventional InP/InGaAsP heterostructures have a relatively low vertical index contrast (typically 3.4 : 3.2). With such materials it does not seem possible to design a compact grating coupler with high efficiency. However, another type of compact grating coupler was proposed in refs. 16 and 17, which uses deeply etched angled grooves instead of shallow rectangular grooves. Because the angle of the grooves is approximately 45°, the fabrication of this type of coupler is more complex and will not be discussed in this paper.

3. Experimental Results of SOI

3.1 Fabrication

The structures were fabricated on 200 mm SOI wafers. The wafers were purchased from SOITEC and have a 220 nm thin silicon top layer and a 1 μm thick buried oxide layer. The total wafer thickness is approximately 750 μm. It should be noted that the thickness of the buried oxide layer is not optimal for grating couplers, but customized wafers are not available in small volumes.

For the fabrication of the grating couplers and waveguides we used deep UV lithography with an illumination wavelength of 248 nm and a numerical aperture of $NA = 0.63$. With these settings, we can, in practice, fabricate periodic structures with a period as low as 400 nm with a sufficiently large process window.[18)]

The process flow of the lithography can be summarized as follows. First, the wafer is coated with Shipley UV3 photoresist and is prebaked. On top of the resist, an antireflective coating is spun to avoid reflection. Then, the wafer is sent to the stepper-scanner, which illuminates the photoresist with a pattern on the mask. On the 200 mm wafer, the die with a pattern is reproduced many times across the wafer. For research purposes, the exposure dose can be varied across the wafer to obtain samples with slightly different linewidths or hole sizes. After lithography, there follows a postexposure bake and development of the resist. The developed photoresist is used as a mask for etching. More details about deep UV lithography can be found in ref. 18.

For the fabrication of photonic integrated circuits with grating couplers, two lithography and etch steps are needed. First, the gratings are defined and etched 70 nm deep. In the second step, the waveguides and circuits are defined and etched 220 nm deep. A scanning electron microscope (SEM) image of such a coupler is shown in Fig. 10.

3.2 Measurement results

To measure the coupling efficiency, we performed transmission measurements on a waveguide with a grating coupler at both ends. An adiabatic taper is used to connect the 12 μm wide input and output waveguides to a single-mode photonic wire (Fig. 1). The length of the tapers is 400 μm, the wide waveguides are 12 μm wide, and the width of the photonic wire is 450 nm. The total distance between the two grating couplers is 3 mm. Cleaved fibers are used for input and output and the fibers are mounted on precision 3-axis translation stages. The angle θ between the fiber axis and the vertical axis is 10°. A widely tunable laser with polarization maintaining output fiber is connected to the input fiber. The output fiber is connected to a power detector. From the transmitted power T, the coupling efficiency η of one coupler can be easily determined because the input and output coupling efficiencies to fiber are the same:

$$T = \eta_{\text{in}}\eta_{\text{out}} = \eta^2 \Rightarrow \eta = \sqrt{T} \tag{3.1}$$

The small propagation losses in the waveguides and tapers are neglected in this equation, and this results in a slight underestimation of the efficiency. For the initial alignment, a camera with a 10x microscope objective lens is used to position the fibers above the gratings. Active alignment at a fixed wavelength is used for the final alignment. There is a

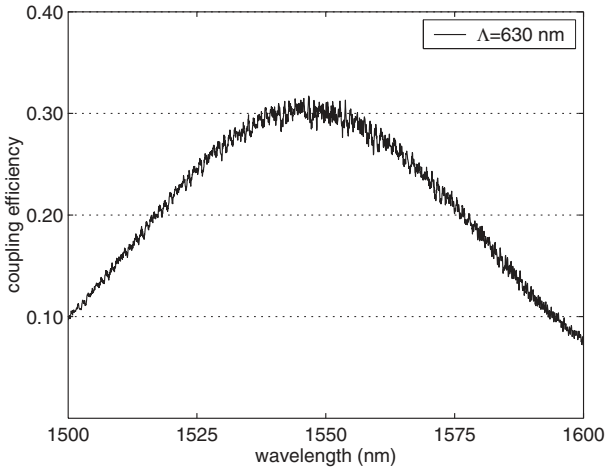

Fig. 11. Measurement result of coupling efficiency as function of wavelength for the coupler shown in Fig. 10.

distance of approximately 11 μm between the grating and the fiber core, because we used straight-cleaved fibers mounted at an angle of 10°. To reduce this distance, angle-cleaved or polished fibers should be used.

The maximum transmission measured is approximately −10.2 dB or 9.6%. This transmission figure includes two couplers. Thus, the coupling efficiency for one coupler is −5.1 dB or 31%. The measured 1 dB bandwidth is approximately 40 nm. The relationship between coupling efficiency and wavelength is shown in Fig. 11. The grating period is 630 nm. Compared with the simulation results, the experimental efficiency is slightly lower and there is also a small wavelength shift, but the results are in good agreement. We also deposited a 750 nm thick oxide cladding on top of some SOI samples. We measured a 34% efficiency for those samples; this is only a slight increase in efficiency and lower than expected. We have also measured the sensitivity to lateral alignment errors of the fiber. During this measurement, the position of the fiber was changed, but the distance between the fiber and the grating was kept constant. The result is shown on Fig. 9. The measurements agree with the simulation results that are also drawn on Fig. 9. An alignment error of 1 μm in any direction results in less than 0.5 dB additional coupling loss.

Although higher experimental coupling efficiencies have already been reported for grating couplers in single-mode SOI slab waveguides, no values of the bandwidth were reported in those papers. In ref. 4, an efficiency of 40% was reported for a beam radius of 14 μm, and the grating couplers were used to characterize integrated waveguides and components. A measured coupling efficiency of 57% has been published in ref. 5, but the cited efficiency is for a Gaussian beam with waist radius $w_0 = 24\,\mu\text{m}$. When comparing these results, it should be noted that our results were obtained using fiber (with a beam radius of 5.2 μm).

4. Indium Phosphide Membrane

4.1 Rationale

SOI is very well suited for components with passive optical functionality, but it is very difficult to make active components in SOI. In indium phosphide (InP)-based compound semiconductors, both active and passive functions can be implemented. However, the vertical index contrast of a conventional InP/InGaAsP heterostructure is too low for making waveguides with a strong vertical confinement, as can be done in SOI. By applying a wafer bonding technique, the vertical index contrast can be modified, resulting in an InP membrane with a high vertical index contrast. These membrane components can then be integrated with conventional InP/InGaAsP-heterostructure active components. To demonstrate the membrane approach, we designed and fabricated compact and efficient grating couplers in InP membranes.

4.2 Design

In our InP membrane approach, first the couplers and waveguides are fabricated and then they are bonded to a host substrate using a low index polymer benzocyclobutene (BCB). Hence, the grating is at the bottom side of the waveguide after bonding. The design method is the same as for SOI-couplers, but we can now choose the BCB-layer thickness to maximize the upwards radiated power. The membrane thickness is 300 nm and the optimized grating parameters are period = 660 nm, etch depth = 120 nm, BCB thickness = 1.18 μm. The coupling efficiency for this structure is 34%. The ratio between the power coupled upwards and downwards can be further increased by adding a layer on top of the InP waveguide core. We use an Al_2O_3 layer ($n = 1.58$), with an optimal thickness of 260 nm. The maximum coupling efficiency is increased to 54%.

4.3 Fabrication

As a first step, the gratings and waveguides are defined by electron-beam lithography using a poly(methyl metacrylate) (PMMA) resist. The layer structure consists of a 300 nm InP membrane layer on top of an InGaAsP etch stop layer on an InP substrate. The pattern is then etched into a FOX-14 (flowable oxide) hard mask and finally into the InP by reactive ion etching (RIE). After removal of the hard mask, the sample is bonded upside-down onto a host substrate by means of BCB.[19] After curing of the BCB at 250 °C for 1 hour, the original InP substrate is removed by lapping and wet etching. Then the etch stop layer is removed by wet etching. Finally the Al_2O_3 layer is deposited on top of the exposed InP waveguide. A SEM cross section of a fabricated structure is shown in Fig. 12.

4.4 Measurements

First, measurements were performed on grating couplers without the top Al_2O_3 coating. The measured coupling efficiency is 19%. The coupling efficiency is increased to 30% when applying a 240 nm Al_2O_3 layer. The coupling efficiency as a function of wavelength is shown in Fig. 13. The discrepancy with the theoretical values (34 and 54% without and with Al_2O_3 coating, respectively) can be attributed to a deviation of the actual structure from the targeted structure. The most important factors are the deviations in BCB thickness and in refractive index of the Al_2O_3 layer from the theoretical values. After measuring the actual parameters of the grating with a SEM (a cross section was made by focused ion beam etching) and the refractive index of the Al_2O_3 layer, the discrepancy between theory and experiment becomes much smaller (Fig. 13). Work is

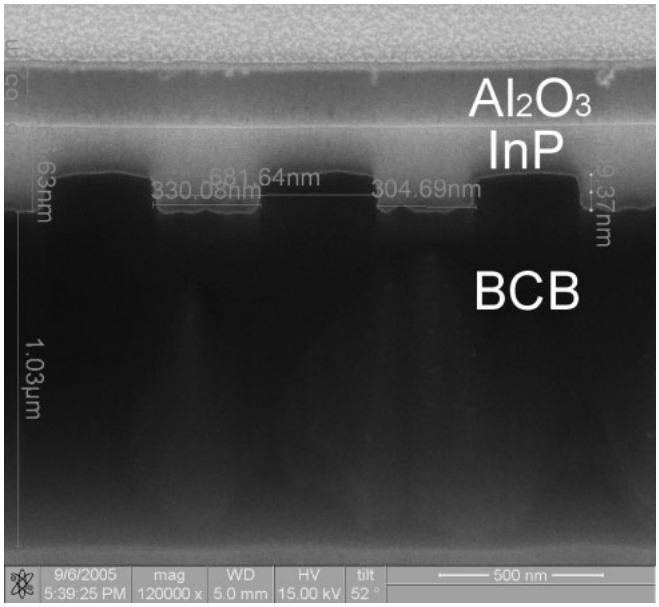

Fig. 12. Cross section of fabricated InP membrane coupler. The InP core layer and the Al_2O_3 and BCB cladding layers are indicated on the SEM image.

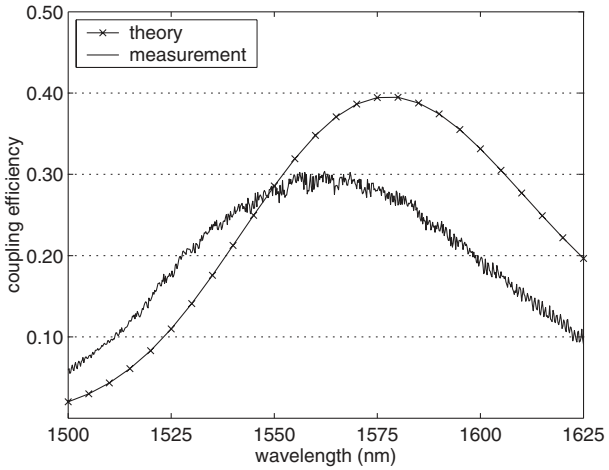

Fig. 13. Measurement result of coupling efficiency of InP membrane coupler and comparison with simulation result.

currently in progress to fabricate the couplers with a gold mirror under the waveguide to increase the efficiency. The bonding procedure we used is well suited for fabricating a SOI coupler with a mirror under the waveguide. In our first experiments, we measured a coupling efficiency of 69% on a coupler with a gold mirror.[20)]

5. Conclusions

We have presented theoretical and experimental results on compact grating couplers for coupling between standard single-mode fibers and integrated waveguides. We have fabricated couplers in SOI and also in InP membranes. These couplers are suitable for the testing of photonic integrated components and circuits. Methods of increasing the coupling efficiency were also discussed but the fabrication of these optimized couplers is more challenging.

Acknowledgements

This work was supported in part by the European Union through the IST-PICMOS, IST-FUNFOX and IST-ePIXnet projects and by the Belgian IAP PHOTON Network. F. Van Laere thanks the Institute for the Promotion of Innovation through Science and Technology in Flanders (IWT-Vlaanderen) for a scholarship. W. Bogaerts acknowledges the Flemish Fund for Scientific Research (FWO-Vlaanderen) for a postdoctoral fellowship. D. Taillaert thanks the Institute for the Promotion of Innovation through Science and Technology in Flanders (IWT-Vlaanderen) for a post-doctoral grant.

1) T. Shoji, T. Tsuchizawa, T. Wanatabe, K. Yamada and H. Morita: Electron. Lett. **38** (2002) 1669.
2) S. J. McNab, N. Moll and Y. A. Vlasov: Opt. Express **11** (2003) 2927.
3) T. Suhara and H. Nishihara: IEEE J. Quantum Electron. **22** (1986) 845.
4) S. Lardenois, D. Pascal, L. Vivien, E. Cassan, S. Laval, R. Orobtchouk, M. Heitzmann, N. Bouzaida and L. Mollard: Opt. Lett. **28** (2003) 1150.
5) R. Orobtchouk, A. Layadu, H. Gualous, D. Pascal, A. Koster and S. Laval: Appl. Opt. **39** (2000) 5773.
6) P. Dinesen and J. Hesthaven: J. Opt. Soc. Am. A **18** (2001) 2876.
7) D. Taillaert, W. Bogaerts, P. Bienstman, T. Krauss, P. Van Daele, I. Moerman, S. Verstuyft, K. De Mesel and R. Baets: IEEE J. Quantum Electron. **38** (2002) 949.
8) D. Taillaert, H. Chong, P. Borel, L. Frandsen, R. De La Rue and R. Baets: IEEE Photonics Technol. Lett. **15** (2003) 1249.
9) S. Peng, T. Tamir and H. Bertoni: IEEE Trans. Microwave Theory Tech. **23** (1975) 123.
10) V. Sychugov, A. Tishchenko, B. Usievich and O. Parriaux: Opt. Eng. **35** (1996) 3092.
11) P. Bienstman and R. Baets: Opt. Quantum Elctron. **34** (2002) 523.
12) D. Taillaert, P. Bienstman and R. Baets: Opt. Lett. **29** (2004) 2749.
13) M. K. Emsley, O. Dosunmu and M. S. Unlu: IEEE J. Sel. Top. Quantum Electron. **8** (2002) 948.
14) K. A. Bates, L. Li, R. L. Roncone and J. J. Burke: Appl. Opt. **20** (1993) 2112.
15) R. Waldhausl, B. Schnabel, P. Dannberg, E. Kley, A. Brauer and W. Karthe: Appl. Opt. **36** (1997) 9383.
16) B. Wang, J. Jiang and G. Nordin: Opt. Express **12** (2004) 3313.
17) F. Van Laere, D. Taillaert, M. V. Kotlyar, D. Van Thourhout, T. F. Krauss and R. Baets: Proc. 31st European Conf. Optical Communications (ECOC 2005), Vol. 2, p. 249.
18) W. Bogaerts, R. Baets, P. Dumon, V. Wiaux, S. Beckx, D. Taillaert, B. Luyssaert, J. Van Campenhout, P. Bienstman and D. Van Thourhout: J. Lightwave Technol. **23** (2005) 401.
19) I. Christiaens, G. Roelkens, K. De Mesel and D. Van Thourhout: J. Lightwave Technol. **23** (2005) 517.
20) F. Van Laere: to be published.